# Using Neural Networks for Predicting the Likelihood of Interference to Groundwave Users in the HF Spectrum

Haris Haralambous
Frederick Institute of Technology,
7 Y. Frederickou Str., Palouriotisa,
1036 Nicosia, Cyprus
H.Haralambous@fit.ac.cy

Harris Papadopoulos
Frederick Institute of Technology,
7 Y. Frederickou Str., Palouriotisa,
1036 Nicosia, Cyprus
H.Papadopoulos@fit.ac.cy

Lefteris Economou
Intercollege
92 Ayias Phylaxeos Str.,
3507 Limassol, Cyprus
leconomou@lim.intercollege.ac.cy

## Abstract

*This paper presents the application of Neural Networks as a means of optimising the reliability of HF groundwave communication systems by predicting the detrimental effect of interference from other users. In the design and performance evaluation of such systems, it is essential to use realistic models of co-channel interference. In response to this demand, the development of a long-term prediction model for the likelihood of interference in the lowest part of the HF spectrum is described. This model can be used in the absence of system capability to assess interference background in real time or near real time, in the context of real time channel evaluation (RTCE), to advise operators on typical interference occupancy levels and assist in the planning of frequency usage and management.*

## 1. Introduction

The HF radio spectrum (3-30MHz) is used extensively for a wide range of communication needs and for all ranges of transmission and provides a means to communicate over long distances with a minimum of infrastructure. Radio communications using this frequency band are referred to as HF communications. The lower limit is sometimes extended below the formal definition, down to 1.6 MHz, when using the term HF communications. Two major propagation mechanisms exist for radio waves in the HF band: Groundwave, where the waves propagate along the surface of the earth, and skywave, where the waves are reflected back to earth from the ionosphere. The groundwave component is utilized in both military and civilian applications, however since attenuation increases with increasing frequency the ground wave is only of use on the lowest part of the spectrum from 1.6 to 4 MHz and for propagation ranges depending on the conductivity of the surface of the earth [8, 3]. The largest conductivity is found at sea, where radio waves at 3 MHz can propagate up to about 500 km.

A potential problem affecting the propagation of groundwave signals is skywave signals which due to their long-range nature give rise to co-channel interference emanating from distant transmitting stations. During daytime, on the lower frequencies below 4 MHz, skywave signals are generally absorbed by the D layer of the ionosphere. In the absence of this layer during night-time, propagation via the F layer can lead to severe co-channel interference. This is a limiting factor in groundwave communication system performance. Under these circumstances, successful communications may depend on finding windows in the frequency band where the interference level is acceptable, or adapting particular system parameters to adequately overcome the interference limitation. The proposed neural network model may be used in conjunction with frequency predictions to advise groundwave HF system operators on typical spectrum occupancy levels and assist in the procedures for estimating communications reliability. The interference measurements used for the model development is part of the dataset obtained in the frames of a long-term project being undertaken jointly by UMIST (University of Manchester Institute of Science and Technology) and by the Swedish Defence Research Establishment, to measure sys-
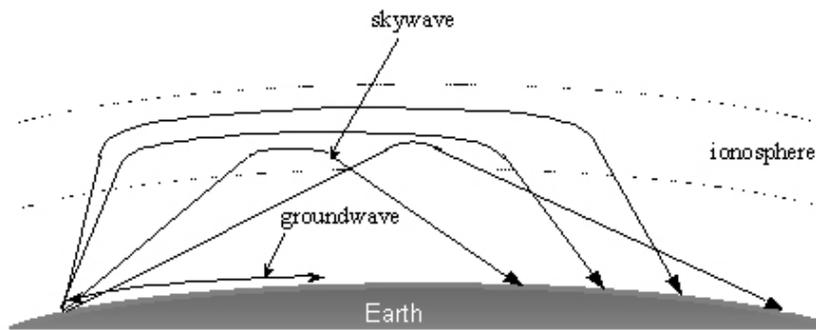
**Figure 1. HF Communication Modes.**

tematically and to analyse the interference of the entire HF spectrum [7, 4].

## 2. HF Communications and Characteristics

### 2.1. Groundwave Propagation

Groundwave propagation occurs when the receiving station is sufficiently close to the transmitting station, and is able to receive the portion of the transmitting station's signal which propagates along the surface of the earth. The range of groundwave propagation varies with the type of antenna at the transmitting station, the characteristics of the ground between the transmitting station and the receiving station, and other factors. Under normal conditions, a groundwave signal propagating over land becomes unusable beyond a radius of 80 kilometres. This range is typically much less due to the actual ground terrain conditions. Distances beyond the range of the groundwave signal are covered by skywaves. By exploiting the ability of the ionosphere to reflect HF signals, skywaves radiate upward at some angle from the antenna, and are reflected from the ionosphere, to allow long-distance propagation (Figure 1). This property may enable the reception of unwanted interference, capable of severely degrading groundwave system performance. Groundwave communications are more straightforward than skywave since the groundwave can be considered an attenuated, delayed but otherwise undistorted version of the transmitted signal [8].

### 2.2. The ionosphere

The ionosphere is defined as a region of the earth's upper atmosphere where sufficient ionisation can exist to affect the propagation of radio waves in the frequency range
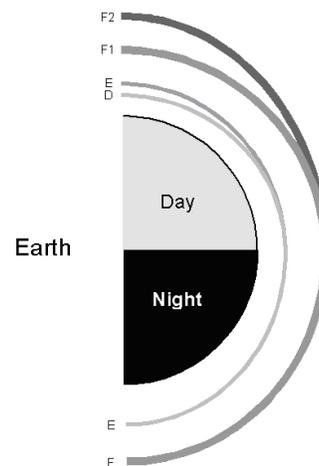


**Figure 2. The layers of the ionosphere.**

1 to 30 MHz. It ranges in height above the surface of the earth from approximately 50 km to 200-600 km. The gases are partially ionised, the level of ionisation at various altitudes being governed by the intensity of the solar radiation and the ionisation efficiency of the neutral gases in the atmosphere. The influence of this region on radio waves is accredited to the presence of free electrons. The density of free electrons at a given height in the ionosphere depends upon the strength of the solar ionising radiation and is therefore a function of time of day, season, geographical location and solar activity [5, 8, 3].

The ionosphere is divided into three regions called D, E and F as shown in Figure 2. The D layer at an average height of 80 km is the lowest ionised layer with an average thickness of about 10 km. It acts mainly as a partial absorber causing signal attenuation in the HF spectrum, the

| Code | Frequency Range (MHz) | User Type |
|------|-----------------------|-----------|
| 1 | 1.606 - 1.810 | Fixed and Mobile |
| 2 | 1.810 - 1.850 | Amateur |
| 3 | 1.850 - 2.045 | Fixed and Mobile |
| 4 | 2.045 - 2.300 | Fixed and Mobile |
| 5 | 2.300 - 2.500 | Fixed, Mobile and Broadcast |
| 6 | 2.500 - 2.850 | Fixed and Mobile |
| 7 | 2.850 - 3.155 | Aeromobile |
| 8 | 3.155 - 3.200 | Fixed and Mobile |
| 9 | 3.200 - 3.400 | Fixed, Mobile and Broadcast |
| 10 | 3.400 - 3.500 | Aeromobile |
| 11 | 3.500 - 3.800 | Fixed, Mobile and Amateur |
| 12 | 3.800 - 3.900 | Fixed and Mobile |
| 13 | 3.900 - 3.950 | Aeromobile |
| 14 | 3.950 - 4.000 | Fixed and Broadcast |

**Table 1. User allocation frequencies.**

dB loss being proportional to the square of the reciprocal of the frequency. Since the degree of ionisation depends on the altitude of the sun, this layer is present only at daytime being most intense at midday [5, 8, 3].

The E layer is present at altitudes of around 100 km with an average thickness of 25 km. The ionisation of the E layer is more pronounced at midday but after dark it falls off more slowly than the D layer and may persist through the night [8]. During daylight the E layer acts mainly as an absorber (less so than the D layer) but also reflects HF waves.

The uppermost layer of the ionosphere is the F layer. During daylight it splits into two distinct layers F1 and F2. The F1 layer exists only during daylight at altitudes from around 150 km. At night the F2 layer which starts at around 300 km merges with the F1. The F2 layer is the principal reflecting region for long distance HF communications [5, 8, 3].

## 2.3. Long-distance skywave propagation

The process of returning radio waves from the ionosphere is through gradual refraction in the ionised layers. Increasing electron density in an ionised layer, causes a reduction in the dielectric constant and hence in the refractive index. As shown in Figure 1 a radio wave ascending into the ionosphere will undergo refraction with the wave tending to bend towards the earth. If the electron density of the ionised layers is sufficient, the refracted wave will eventually be parallel to the layer and bent downwards, emerging from the ionised layer at an angle of reflection [8, 3].

Long distances (above 4,000 km) are covered by multi-hop propagation, with the wave reflecting back and forth

several times between the ionosphere and the surface of the earth. The ionosphere will reflect a wave emitted from a transmitting antenna on the ground at vertical incidence to its layers provided that the frequency is not too high. Longer distances are covered by multi-hop propagation, with the wave reflecting back and forth between the ionosphere and the Earth's surface or between different ionospheric layers several times. Figure 3 shows examples of possible two-hop single-path propagation scenarios [8].

## 2.4. HF Spectrum Management

The ionosphere constitutes a worldwide communication medium shared by various types of user. As a result, the HF spectrum is subject to an international agreement on its utilisation. It is divided by the International Telecommunications Union (ITU) into frequency allocations on the basis of the following 9 different types of user [2]:

- Mobile
- Aeromobile
- Fixed
- Broadcast
- Aeronautical Mobile
- Martime Mobile
- Land Mobile
- Amateur
- Standard Frequency

The allocations for each user type are distributed across the HF spectrum so that sky wave communication for a variety of communication ranges and ionospheric propagation conditions can be facilitated. In this paper only 14 allocations at the lower part of the HF spectrum are considered (below 4 MHz) since groundwave propagation is primarily limited in this frequency range. These ITU defined HF allocations were interpreted in accordance to the measurement of spectral occupancy and their respective frequency ranges are shown in Table 1 [7].

## 3. Interference Data and Characteristics

The dataset of diurnal occupancy measurements used for the model development was taken over a period of seven years (April 1994 to January 2000) in the frames of a long-term project being undertaken jointly by UMIST and by the Swedish Defence Research Establishment, to measure systematically and to analyse the occupancy of the entire
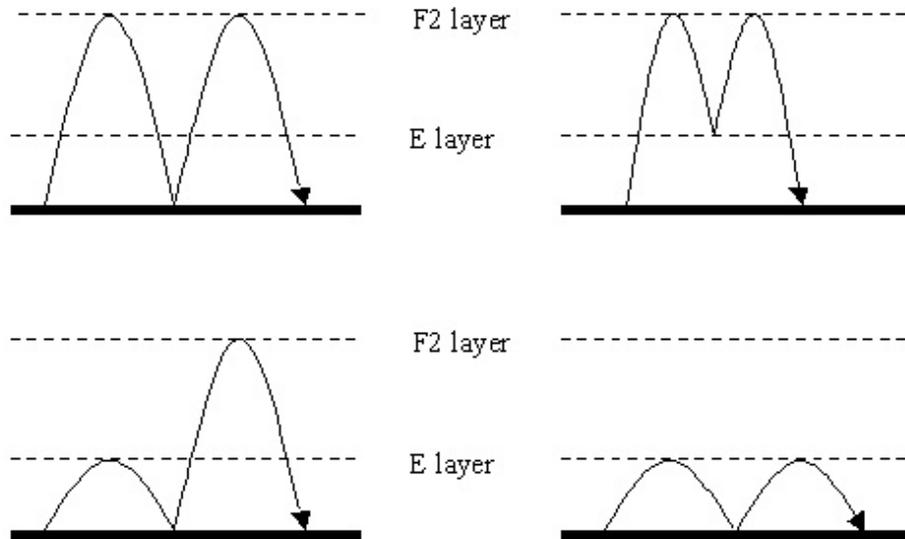
**Figure 3. Examples of possible two-hop propagation paths.**

HF spectrum over Northern Europe [7, 4]. The measure of occupancy used is congestion, which is defined to be the probability of placing at random, a bandpass filter of a given bandwidth in a given ITU defined frequency allocation, such that the RMS value of the filter output signal exceeds a predefined threshold level [6, 9, 10].

Diurnal measurements of occupancy were typically obtained once a week. One measurement session was carried out by stepping a filter of 1 kHz bandwidth in frequency increments of 1 kHz through each of the 95 ITU user defined allocations, spending 90ms at each increment. The fraction of the allocation spectral width for which the RMS signal level at each step exceeded a defined field-strength threshold level was determined. This defines the congestion Q for that allocation, for the corresponding threshold level [7]. Therefore for 95 user allocations, one complete measurement of the HF spectrum resulted in $95 \times 5 \times 24 = 11400$ experimental congestion values, which constitutes a complete diurnal measurement. However in this paper, only 14 allocations are considered in the modeling process so the congestion values per measurement taken into account are 1680. The total number of measurement sessions that were carried out is 197 which corresponds to a total of 330960 congestion values. The measurement antenna was a calibrated active monopole, which gives a constant output voltage for a constant incident field strength, across the entire HF spectrum. Referred to the antenna input terminal, the range of measurement threshold levels used is -117dBm to -77dBm, in 10dB increments. Figure 4 shows an example of a congestion measurement, with signal threshold levels superimposed.

During daylight, the typical window of operating frequencies will be somewhere in the middle of the HF spectrum, whereas at night, the operating window will shift to the lower portion of the spectrum. This is due to the lack of ionospheric support at higher frequencies and the absence of D-layer absorption at night. Previous research [7] on the occupancy of the HF spectrum, shows that the lower part of the HF band is severely congested, particularly at night. This is illustrated in Figure 5, which shows typical recorded HF spectra for day and night periods. Similar behaviour for the measured occupancy is illustrated in Figure 6. In Figure 7 the diurnal variation of the measured occupancy of the entire HF spectrum is depicted and Figure 8 illustrates the same variation for a single allocation at different signal threshold levels. The seasonal variation of congestion in an allocation is clearly shown in Figure 9.

## 4. Model Parameters

The variation of occupancy of the HF specrum due to skywave signals is primarily dependant on prevailing ionospheric conditions. The input parameters for modelling congestion were selected so as to represent the known variations that give rise to the most characteristic properties of the ionosphere as a communications channel.

A short-term strong dependency between interference and the hour of the day is clearly evident by observing Figure 8. We therefore include hour numbers in the inputs to the NN. The hour number, $hour$, is an integer in the range
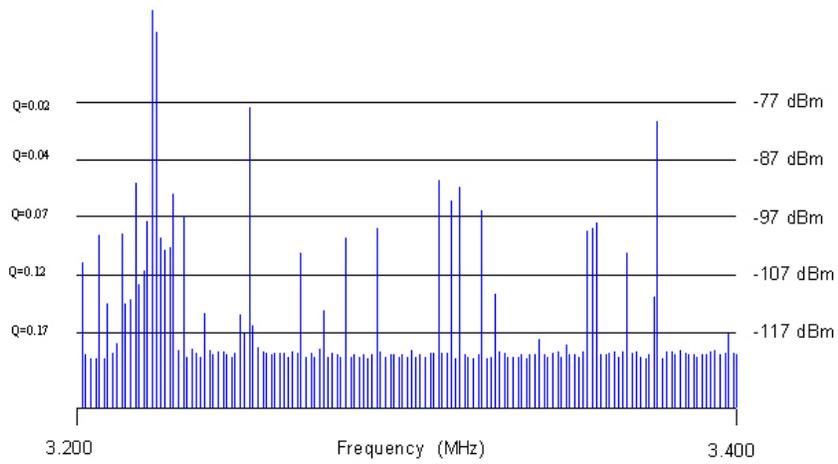
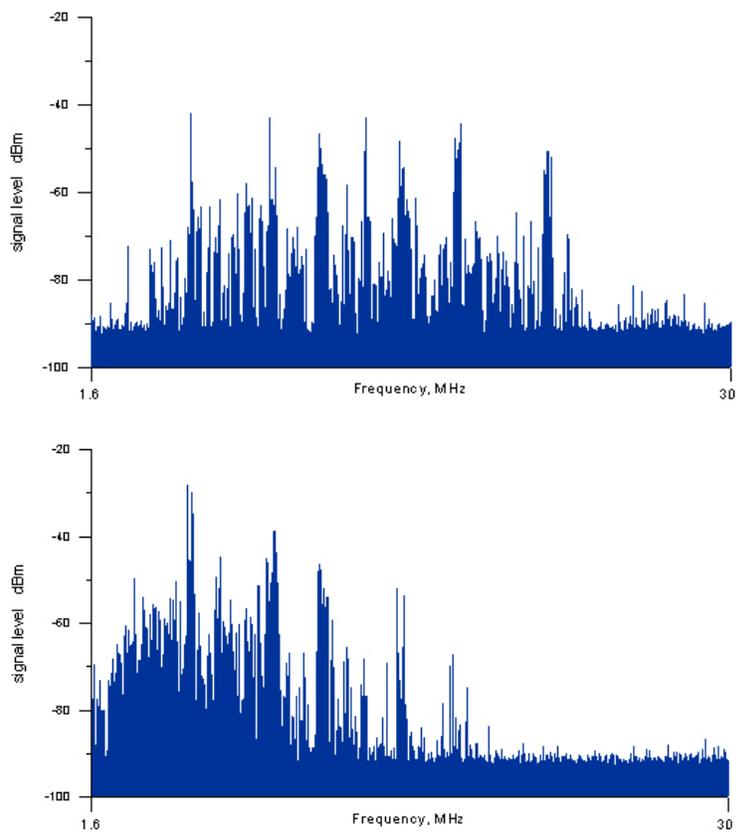**Figure 4. Signal measurements taken within an ITU allocation.**



**Figure 5. Typical recorded day (top) and night (bottom) spectra.**
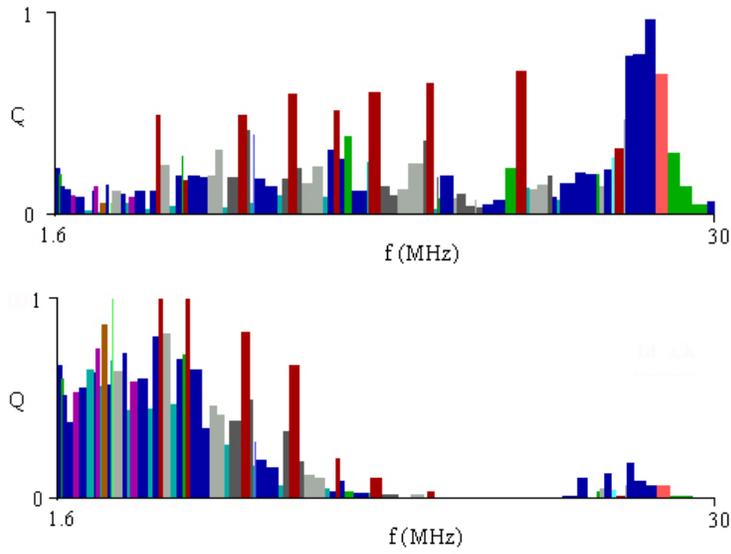
**Figure 6. Examples of measured day (top) and night (bottom) congestion at the -117 dBm signal threshold level.**
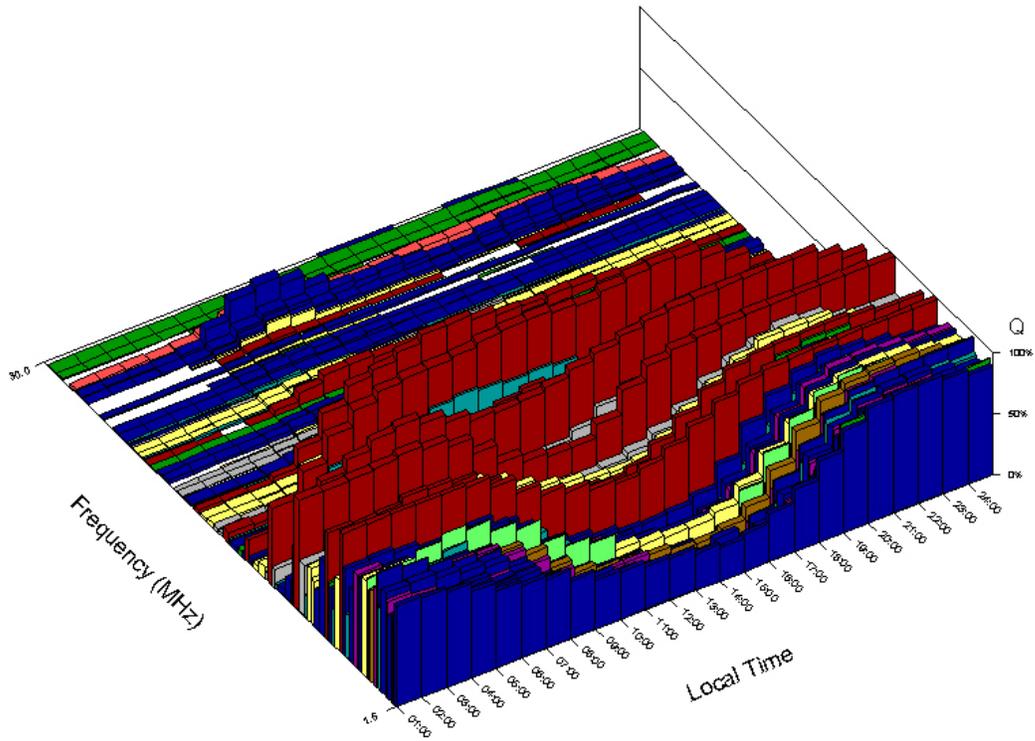


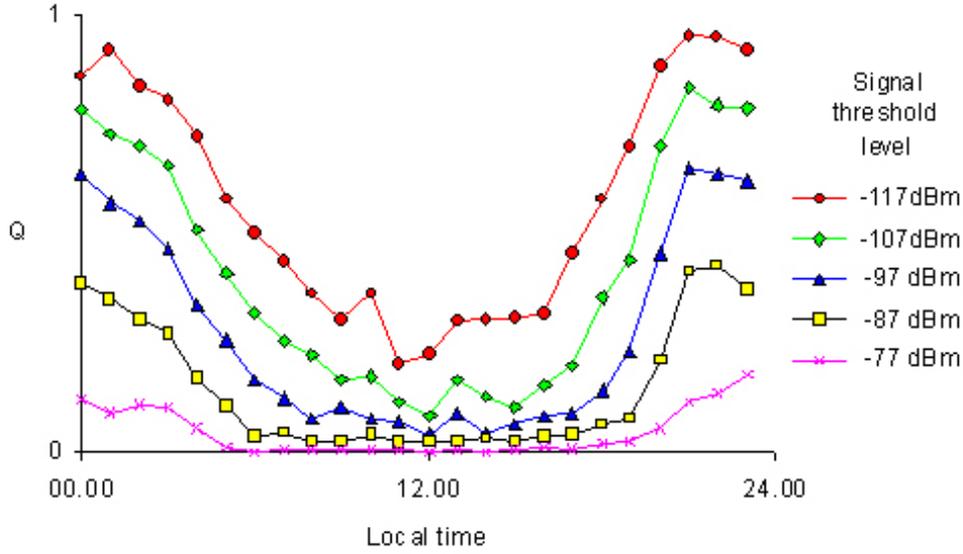**Figure 7. Diurnal variation of measured occupancy of the HF Spectrum.**

**Figure 8. Examples of diurnal variation of measured congestion at different signal threshold levels within an allocation.**

$0 \leq hour \leq 23$. In order to avoid unrealistic discontinuity at the midnight boundary, hour is converted into its quadrature components according to

$$sinhour = sin\left(2\pi\frac{hour}{24}\right) \qquad (1)$$

and

$$coshour = cos\left(2\pi\frac{hour}{24}\right). \qquad (2)$$

A seasonal variation clearly shown in Figure 9 is described by day number $daynum$ in the range $1 \leq daynum \leq 365$. This variation is due to the response of the critical frequency of the F2 layer, which acts as the principal reflector of radiowaves in the ionosphere for long-distance transmission, to the seasonal change in extreme ultraviolet (EUV) radiation from the Sun. Again to avoid unrealistic discontinuity between December 31st and January 1st $daynum$ is converted into its quadrature components according to

$$sinday = sin\left(2\pi\frac{daynum}{365}\right) \qquad (3)$$

and

$$cosday = cos\left(2\pi\frac{daynum}{365}\right). \qquad (4)$$

Solar activity has an impact on ionospheric dynamics which in turn influence the electron density of the ionosphere. This directly affects the critical frequency of layer F2 which is proved to be highly correlated with congestion [7]. The solar activity varies with a periodicity of approximately eleven years. This long-term variation was included as a separate input parameter with a running mean value of the daily sunspot number (R) which is a well established index of solar activity [1]. After a thorough investigation a 50-day running mean value of the daily sunspot number $R50$ was found to be the optimum parameter to represent the long-term variation of congestion.

Signal threshold level is also incorporated as an input parameter ($ST$) since it is obvious from Figure 8 that it has a profound effect on measured congestion. This is quite reasonable since increasing the threshold would normally correspond to fewer channels exceeding its value so this would result in a lower congestion value.

## 5. Results

In our experiments each neural network was trained to predict the congestion of a given allocation based on the $sinhour$, $coshour$, $sinday$, $cosday$, $R50$ and $ST$ parameters. As mentioned in Section 3 the data used consisted of 23640 congestion values for each of the 14 allocations. These values were recorded in 197 measurement sessions which were carried out once a week. Each session recorded the congestion values of all allocations with respect to each of the five threshold levels every hour of the day the measurement took place; thus each measurement session re-
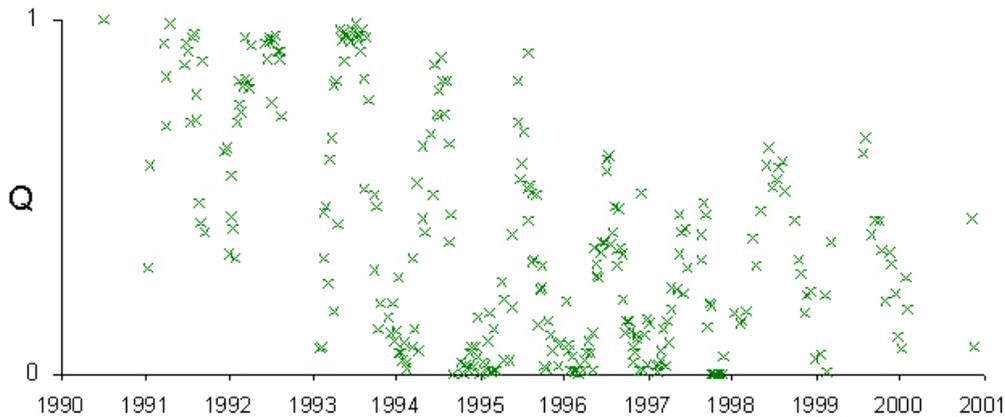
**Figure 9. Examples of seasonal variation of night measured congestion at the -117 dBm signal threshold level.**

sulted in $24 \times 5 = 120$ congestion values for each allocation.

All networks used had exactly the same structure. They were fully connected two-layer neural networks, with 6 input, 19 hidden and 1 output neurons. Both their hidden and output neurons had logistic sigmoid activation functions. The number of hidden neurons was determined by trial and error on 3 of the 14 allocations. These networks were trained using the Levenberg-Marquardt backpropagation algorithm for 100 epochs. There was no worry of overfitting since the number of free parameters of the networks was very small compared to the number of examples used for their training. This can also be observed in Figure 10, which shows a typical learning curve of our experiments.

All inputs to our networks were normalized setting the minimum value of each input to -1 and its maximum value to 1. No normalization was needed for their outputs since they were already in the interval [0, 1].

The experiments were carried out using 10 random splits of the whole dataset into training and test sets. More specifically, for each split 20 out of the 197 measurement sessions were randomly selected to form the test set, and the remaining 177 were used to form the training set; all 120 congestion values of each session were treated as a group and were placed either in the training or in the test set. As a result, there was no temporal correlation between the examples of the training and test sets of each split, since the values of each set were recorded during different measurement sessions. For each of the 14 allocations one neural network was trained and tested on every split and the results reported here were obtained by averaging the results of all 10 splits.

In Table 2 we report the Root Mean Squared Error

| Allocation | RMSE | R |
|---|---|---|
| 1 | 0.067 | 0.946 |
| 2 | 0.084 | 0.900 |
| 3 | 0.063 | 0.944 |
| 4 | 0.061 | 0.941 |
| 5 | 0.061 | 0.950 |
| 6 | 0.057 | 0.962 |
| 7 | 0.060 | 0.938 |
| 8 | 0.075 | 0.947 |
| 9 | 0.059 | 0.965 |
| 10 | 0.063 | 0.928 |
| 11 | 0.058 | 0.968 |
| 12 | 0.064 | 0.947 |
| 13 | 0.068 | 0.910 |
| 14 | 0.095 | 0.946 |

**Table 2. The RMSE and the correlation coefficient (R value) for each allocation.**

(RMSE) and the correlation coefficient (R value) between the network predictions and the measured congestion values for each allocation. Both the low RMSE values and the close to unity correlation coefficient values show that the trained neural networks can successfully predict congestion in the allocations under consideration. This belief is also supported by the plots of measured and predicted congestion values in Figure 11.
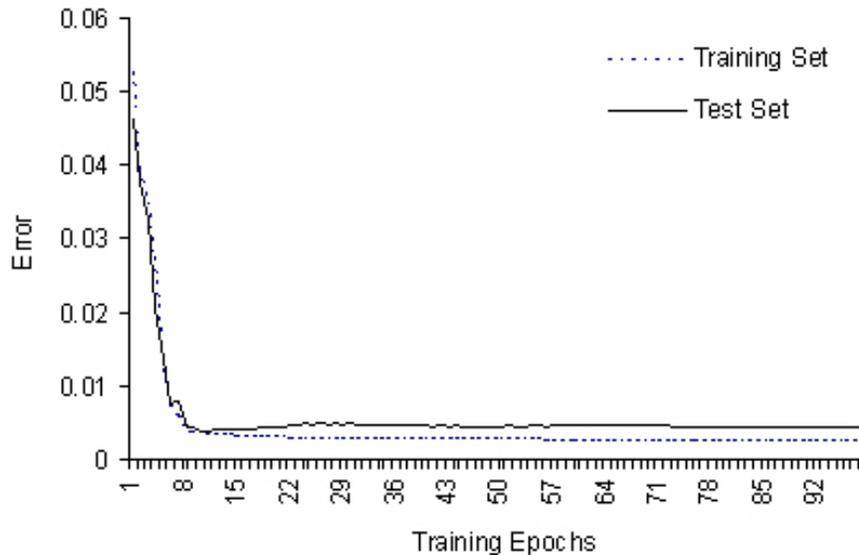
**Figure 10. The learning curve for one of the splits of allocation 7.**

## 6. Conclusions

In this study we have demonstrated the practical application of neural networks to predict the likelihood of interference due to skywave signals, which represents one of the most significant impediments to successful groundwave HF communication. The remarkable agreement between the neural network predicted values and observed congestion data signifies the ability of the resulting networks to provide a quantitative description of the diurnal, seasonal and long-term trend in the variability of congestion.

The proposed networks require the day number, hour, 50-day running mean sunspot number and signal threshold as inputs, and predict the corresponding congestion value, which indicates the likelihood of interference under the given conditions. As a result, it can be a useful tool for HF groundwave users in an attempt to ensure that a satisfactory grade of service is achieved from the point of view of an interference free channel.

## 7. Acknowledgements

## References

[1] World data centre, rutherford appleton laboratory.

[2] Radio regulations revised table of frequency allocations and associated terms and definitions, 1979.

[3] K. Davis. *Ionospheric Radio*. Peregrinus, 1990.

[4] L. Economou, P. Green, G. Gott, P. Laycock, M. Broms, and S. Boberg. Hf spectral occupancy at high latitudes. In *Proceedings of HF98, Nordic Shortwave Conference*, 1998.

[5] J. Goodman. *HF Communications, Science and Technology*. Van Nostrand Reinhold, 1992.

[6] G. Gott, S. Chan, C. Pantjiaros, and P. Laycock. High frequency spectral occupancy at the solstices. *IEE Proceedings Communications*, 144(1):24–32, February 1997.

[7] G. Gott, C. Pantjiaros, J. Wylie, and P. Laycock. Hf spectral occupancy measurements in europe. In *IEE Colloquium on Frequency Selection and Management Techniques for HF Communications*, 1996.

[8] N. Maslin. *HF Communications, a Systems Approach*. Pitman, 1987.

[9] C. Pantjiaros, J. Wylie, J. Brown, G. Gott, and P. Laycock. Development of the laycock-gott occupancy model. *IEE Proceedings Communications*, 144(1):33–39, February 1997.

[10] C. Pantjiaros, J. Wylie, J. Brown, G. Gott, and P. Laycock. Extended uk models for high frequency spectral occupancy. *IEE Proceedings Communications*, 145(3):168–174, February 1998.
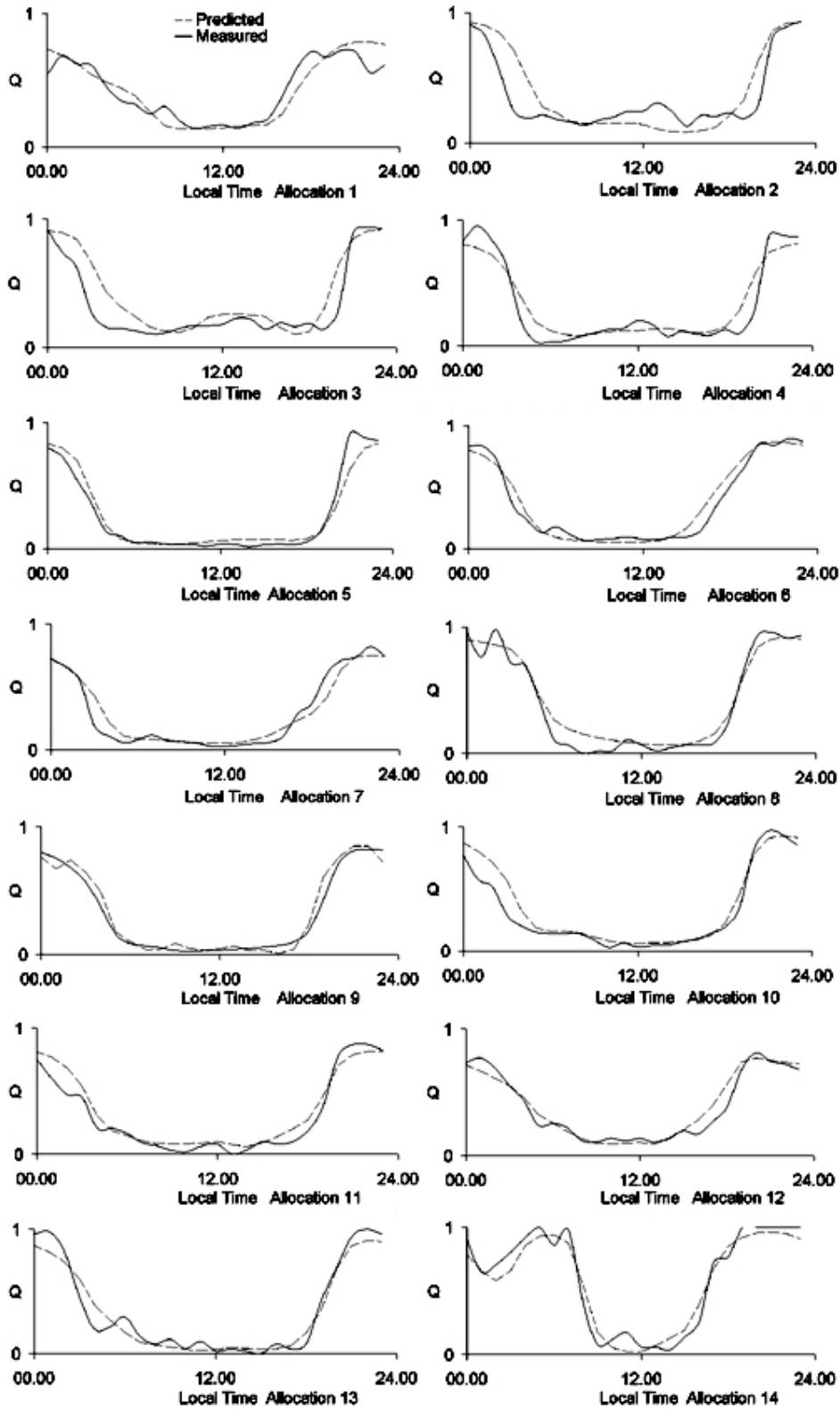
**Figure 11. Examples of diurnal measured and predicted congestion at a signal threshold level of -117 dBm.**